Science Advances

MAAS

Supplementary Materials for

Targeting BRD3 eradicates nuclear TYRO3-induced colorectal cancer metastasis
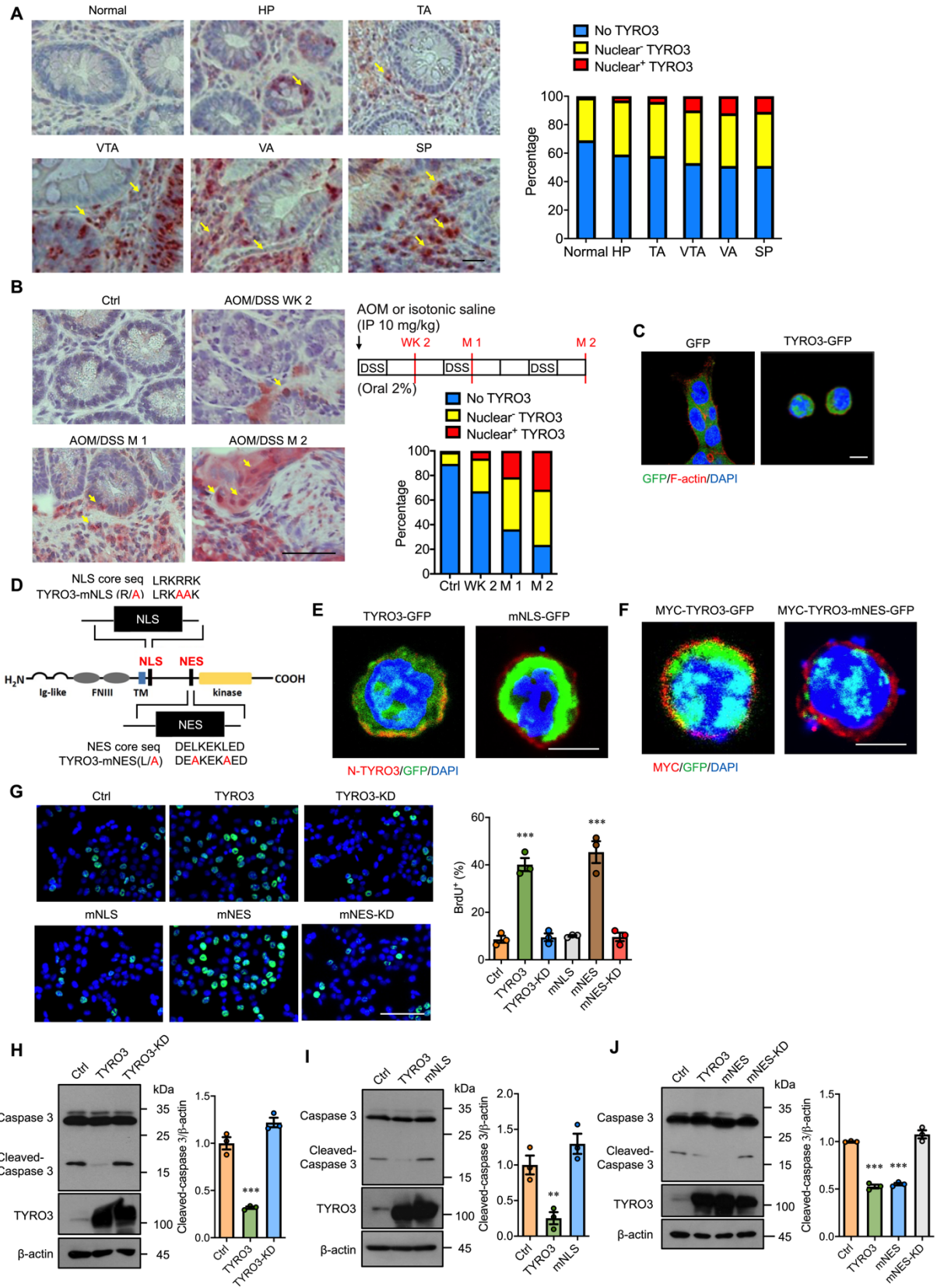
Pei-Ling Hsu *et al.*

Corresponding author: Shaw-Jenq Tsai, seantsai@mail.ncku.edu.tw; H. Sunny Sun, hssun@mail.ncku.edu.tw

This PDF file includes:

Figs. S1 to S7
Table S1

A

Normal | HP | TA
VTA | VA | SP

Percentage

- No TYRO3 (blue)
- Nuclear⁻ TYRO3 (yellow)
- Nuclear⁺ TYRO3 (red)

Normal HP TA VTA VA SP

B

Ctrl | AOM/DSS WK 2
AOM/DSS M 1 | AOM/DSS M 2

AOM or isotonic saline
(IP 10 mg/kg)
↓
WK 2   M 1   M 2
| DSS | | DSS | | DSS |
(Oral 2%)

- No TYRO3
- Nuclear⁻ TYRO3
- Nuclear⁺ TYRO3

Percentage

Ctrl WK 2 M 1 M 2

C

GFP | TYRO3-GFP

GFP/F-actin/DAPI

D

NLS core seq   LRKRRK
TYRO3-mNLS (R/A)   LRKAAK

NLS

H_2N — Ig-like — FNIII — TM — NLS — NES — kinase — COOH

NES

NES core seq   DELKEKLED
TYRO3-mNES(L/A)   DEAKEKAED

E

TYRO3-GFP | mNLS-GFP

N-TYRO3/GFP/DAPI

F

MYC-TYRO3-GFP | MYC-TYRO3-mNES-GFP

MYC/GFP/DAPI

G

Ctrl | TYRO3 | TYRO3-KD
mNLS | mNES | mNES-KD

BrdU⁺ (%)

*** ***

Ctrl TYRO3 TYRO3-KD mNLS mNES mNES-KD

H

Caspase 3
Cleaved-Caspase 3
TYRO3
β-actin

kDa
35
25
15
100
45

Cleaved-caspase 3/β-actin

***

Ctrl TYRO3 TYRO3-KD

I

Caspase 3
Cleaved-Caspase 3
TYRO3
β-actin

kDa
35
25
15
100
45

Cleaved-caspase 3/β-actin

**

Ctrl TYRO3 mNLS

J

Caspase 3
Cleaved-Caspase 3
TYRO3
β-actin

kDa
35
25
15
100
45

Cleaved-caspase 3/β-actin

*** ***

Ctrl TYRO3 mNES mNES-KD

2

**Fig. S1.**

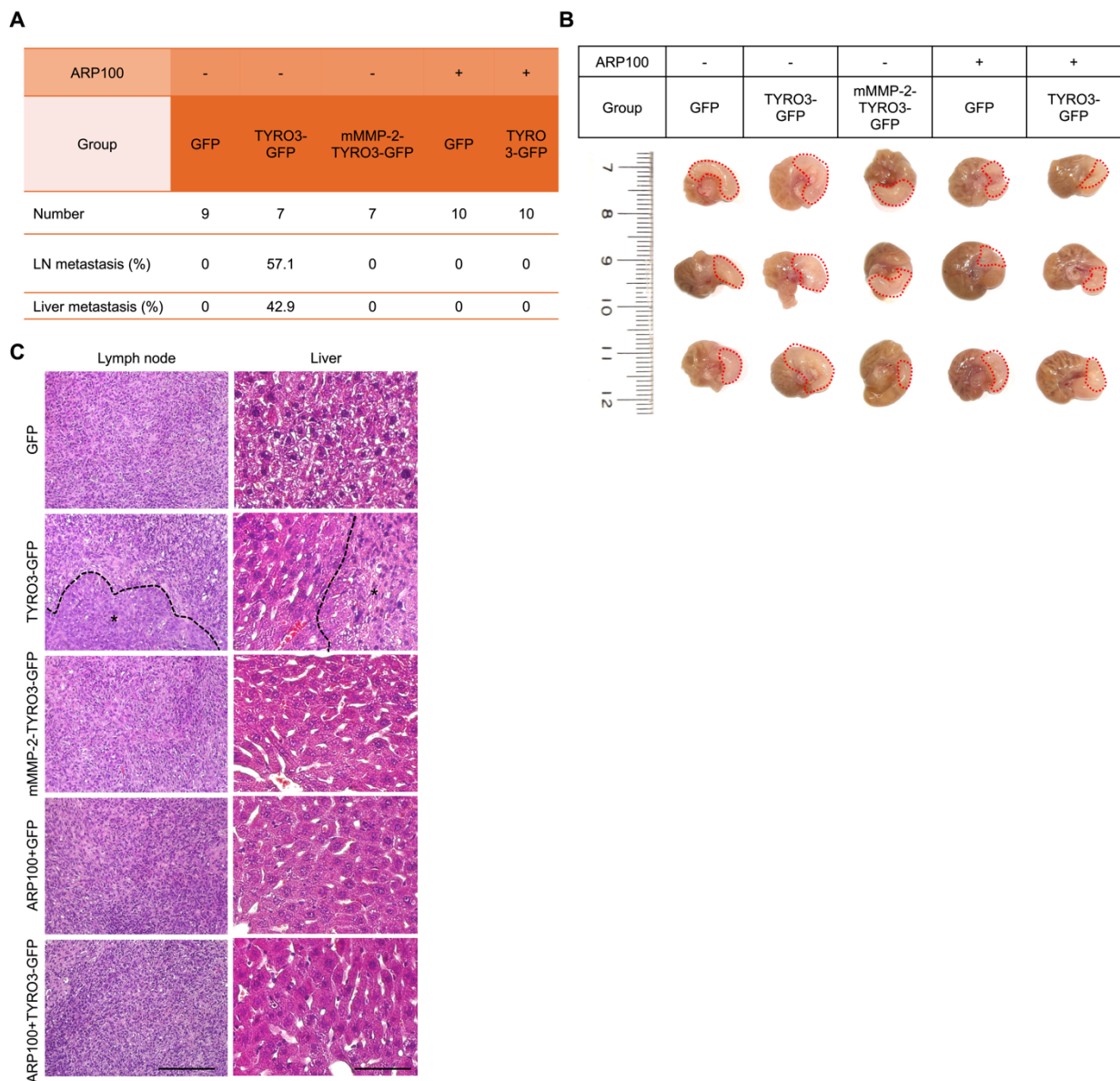**Anti-apoptotic nuclear TYRO3 is induced in the early stage of polyps and CRC in mice.**

(A) Tissue sections from normal and different types of polyps (n = 12) were subjected to TYRO3 staining (red) and counterstained with hematoxylin for nuclei by IHC staining. Scale bar: 50 μm. Numbers are the percentage of TYRO3 subcellular localization in different types of polyps, P < 0 .001. HP, Hyperplastic polyp; TA, Tubular adenoma; VTA, Villo-tubular adenoma; VA, Villous adenoma; SP, Serrated polyp. **(B)** Schematic drawing indicated the experimental protocol to create AOM/DSS-induced colon cancer mouse model (upper right panel). The control group drank water only. TYRO3 expression in the mice 2 weeks, 1 month, and 2 months after AOM treatment was identified by IHC staining (left panel). IP, intraperitoneal injection. Scale bar: 50 μm. The cytosolic and nuclear TYRO3 expression were quantified as percentage (lower right panel, n = 6 mice/time point), $P < 0.05$. **(C)** Images showed location of GFP (green), F-actin (red), and DAPI (blue) after transfection for 24 hours in HCT116 cells. Direct GFP fluorescence was detected. Scale bar: 10 μm. **(D)** Schematic drawing of the localization of the NLS and the NES sequences within TYRO3. The core sequence of NLS was mutated from RKRR to RKAA and RKGG. The amino acid in core sequence of NES was mutated from L to A. Ig-like, immunoglobulin-like domains; FNIII, fibronectin type III; TM, transmembrane region. **(E)** Immunofluorescence staining images showed location of N-terminal TYRO3 (red) and C-terminal TYRO3 (GFP) in SW480 cells. Scale bar: 10 μm. **(F)** Images showed locations of N-terminus (red, MYC) and C-terminus (GFP) of TYRO3 in SW480 cells. Scale bar: 10 μm. **(G)** Representative images (left panel) and quantified result (right panel) of bromodeoxyuridine (BrdU) incorporation assay in SW480 cells (n = 3). Scale bar: 100 μm. Statistical significance was calculated using one-way ANOVA and post-hoc Tukey's tests, ***: $P < 0.001$. **(H-J)** Representative Western blots (left panel) and quantified data (right panel, n = 3) showed the levels of caspase 3, TYRO3, and β-actin in HCT116 cells transfected with the indicated plasmids. Ctrl: empty vector; TYRO3-KD: kinase dead TYRO3; mNLS: NLS mutated TYRO3; mNES: NES mutated TYRO3; mNES-KD: kinase dead mNES-TYRO3. **: $P < 0.01$, and ***: $P < 0.001$.
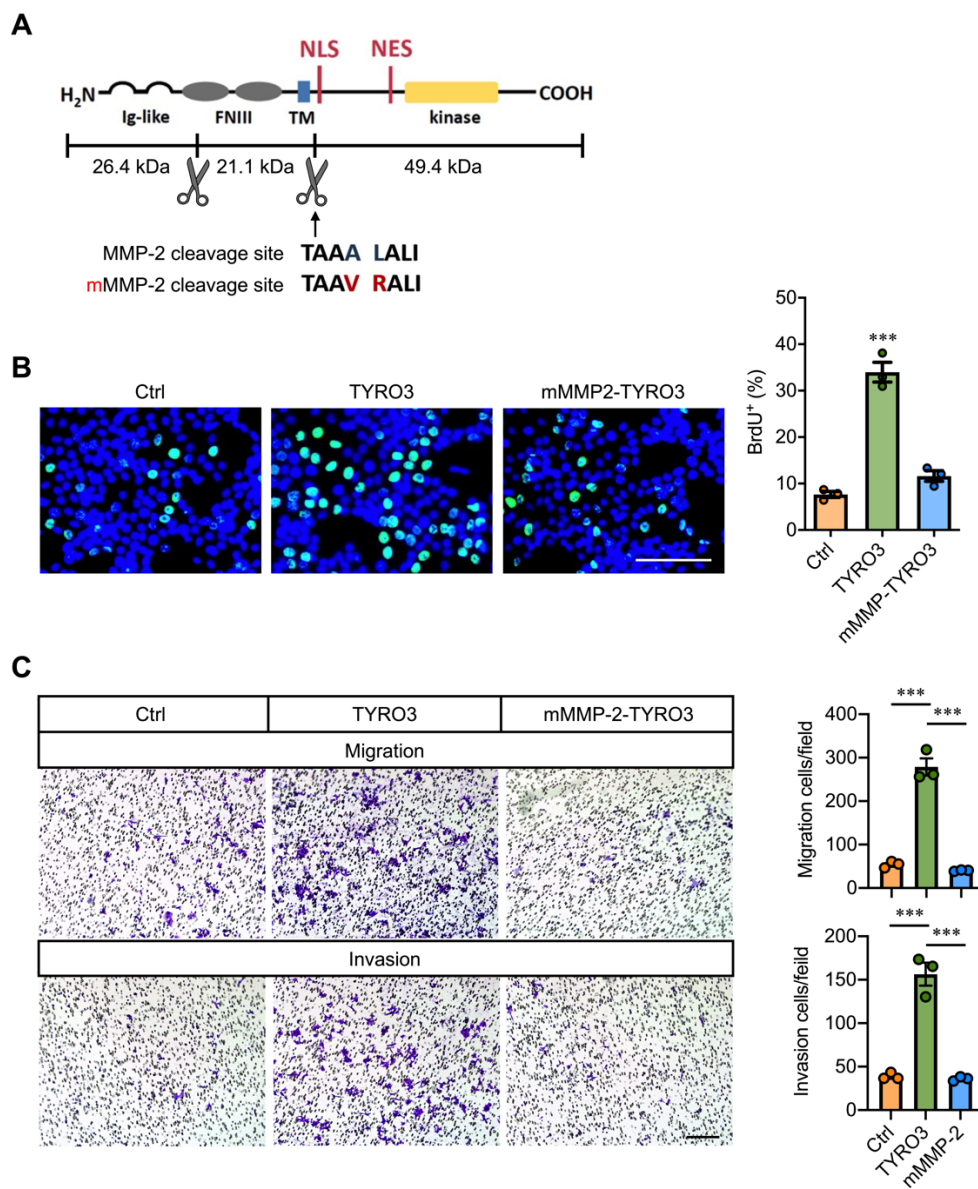
Fig. S2.

**MMP-2 mediates TYRO3-induced colon cancer cell proliferation.**

(A) The cartoon showed the two MMP-2 predictive cleavage sites in TYRO3 and the mutation of MMP-2 cleavage site (mMMP-2) in TYRO3 (mMMP-2-TYRO3). **(B)** Representative images (left panel) and quantified result (right panel) of BrdU incorporation assay (n = 3). Scale bar: 100 μm. Statistical significance was calculated using one-way ANOVA and post-hoc Tukey's tests, ***: $P < 0.001$. **(C)** Transwell migration and invasion assays were performed after transfection of SW480 cells with GFP only (control), TYRO3-GFP (TYRO3), and mMMP2-TYRO3-GFP (mMMP2-TYRO3) plasmids. Representative images (left panel) and quantification results (right panel) are shown (n = 3). Scale bar: 200 μm. ***: $P < 0.001$.

A

ARP100	-	-	-	+	+
Group	GFP	TYRO3-GFP	mMMP-2-TYRO3-GFP	GFP	TYRO3-GFP
Number	9	7	7	10	10
LN metastasis (%)	0	57.1	0	0	0
Liver metastasis (%)	0	42.9	0	0	0

B

ARP100	-	-	-	+	+
Group	GFP	TYRO3-GFP	mMMP-2-TYRO3-GFP	GFP	TYRO3-GFP

C

Fig. S3.

MMP-2 mediates TYRO3-induced CRC malignancy.

(A-C) The orthotopic injection of HCT116 stable cells with overexpression of GFP (n = 9), TYRO3-GFP (n = 7), or mMMP-2-GFP (n = 7) into the NOD/SCID mice with or without ARP100 treatment (5 mg/kg/day, n = 10). (A) The numbers of survival and metastases of mice in all groups. (B) The representative picture showing the lesion in the cecum after 1 month. (C) Lymph node and liver tissue sections were processed for H&E staining. Scale bar: 100 μm, left panel; 50 μm, right panel. Dashed lines delineate the boundaries segregating cancer and normal tissues. Asterisks indicate the cancers.
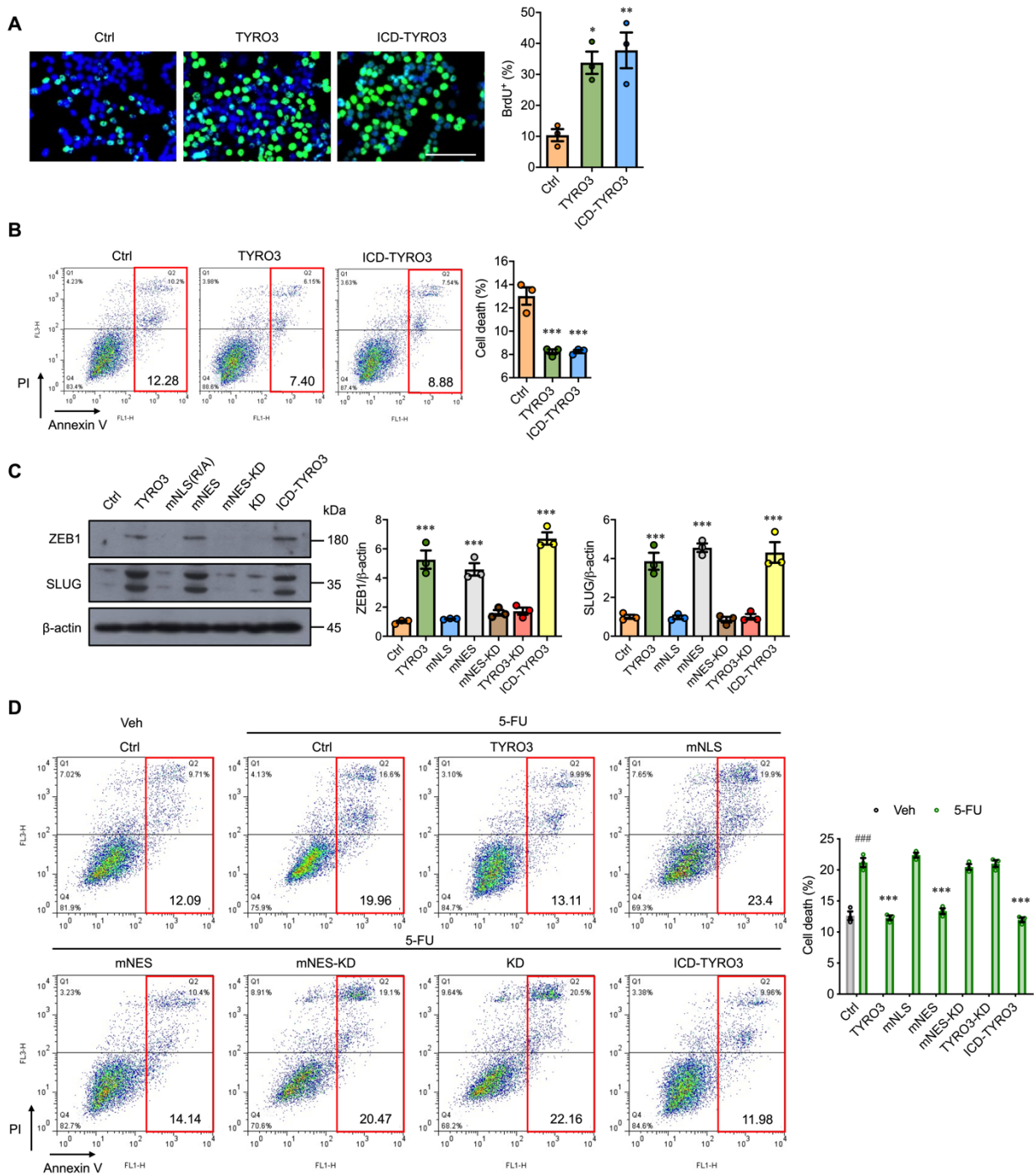
Fig. S4.

Nuclear TYRO3 promotes drug resistance.

(A) Representative images (left panel) and quantified result (right panel) of BrdU incorporation assay (n = 3). Scale bar: 100 μm. Statistical significance was calculated using one-way ANOVA and post-hoc Tukey's tests, *: $P < 0.05$, **: $P < 0.01$. **(B)** Representative images (left panel) and

quantified result (right panel, n=3) show percentage of cell death. Statistical significance was calculated using one-way ANOVA and post-hoc Tukey's tests, ***: $P < 0.001$. **(C)** Representative Western blots (left panel) and quantified data (right panel, n = 3) showed the levels of ZEB1, SLUG, and β-actin in HCT116 cells transfected with the indicated plasmids for 5 days. ***: $P < 0.001$. **(D)** Representative images (left panel) and quantified result (right panel, n=3) show percentage of cell death with 5-FU (80 μg/ml) treatment. Asterisks indicate statistical differences as compared to control group treated with 5-FU and pound sign indicates statistical difference between control group treated with vehicle and control group treated with 5-FU, *** and ###: $P < 0.001$.
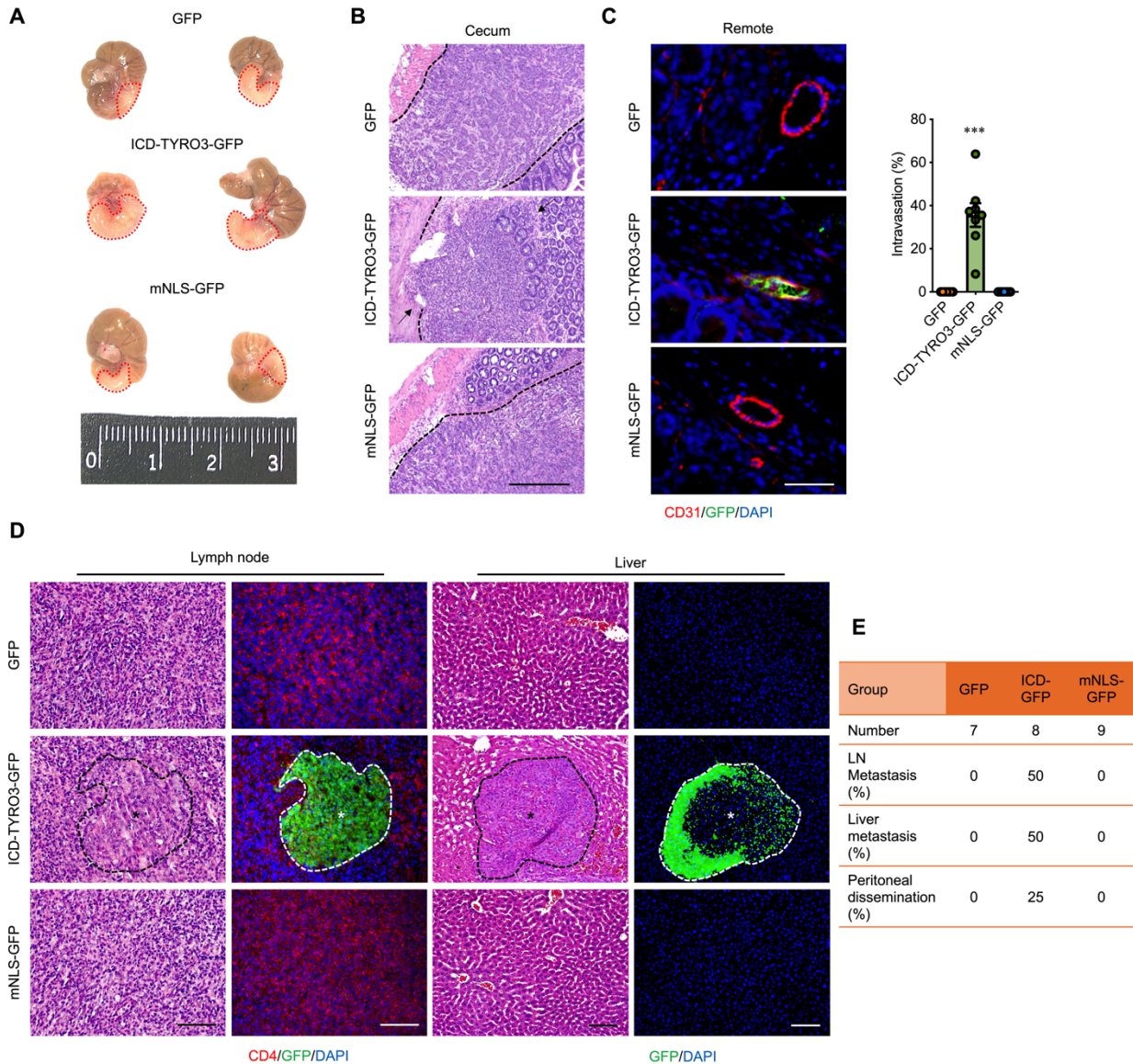
Fig. S5.

Nuclear TYRO3 promotes CRC severity in mice.

(A) Orthotopic implantation was performed using HCT116 stable cell lines with overexpression of GFP, ICD-TYRO3-GFP or mNLS-TYRO3-GFP (mNLS-GFP). The representative picture showing the lesion in the cecum after 1 month. **(B)** Tissue sections were processed for hematoxylin and eosin (H&E) staining. Scale bar: 100 μm. Arrows indicate the invasive cancer. Dashed lines delineate the boundaries segregating cancer and normal tissues. **(C)** Remote area (over 100 μm distance) sections were stained with anti-GFP (green) for cancer cells, anti-CD31(red) for endothelial cells, and counterstained with DAPI. Scale bar: 25 μm. Numbers are the percentage of intravasation at remote area. Statistical significance was calculated using one-way ANOVA and post-hoc Tukey's tests, ***: $P < 0.001$. **(D)** Lymph nodes were stained with H&E or anti-GFP (green) for cancer cells, anti-CD4 (red) for lymphocytes, and counterstained with DAPI. Liver
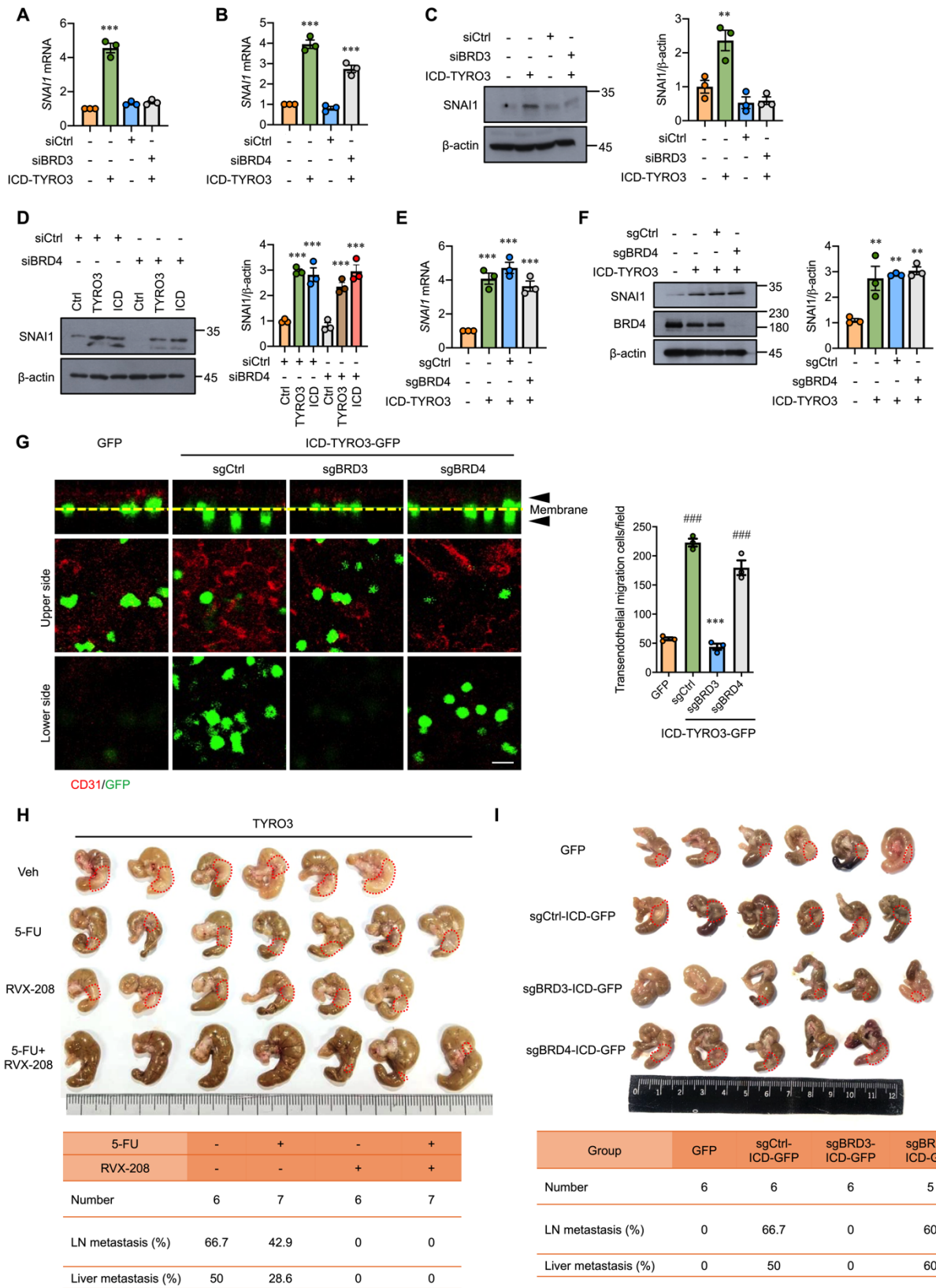
tissue sections were stained with H&E or anti-GFP (green) and counterstained with DAPI. Scale bar: 100 μm. Dashed lines delineate the boundaries segregating cancer and normal tissues. The cancer regions were marked by asterisks. **(E)** The percentages of lymph node invasion, peritoneal dissemination, and liver metastases of mice in all groups were shown in the table.
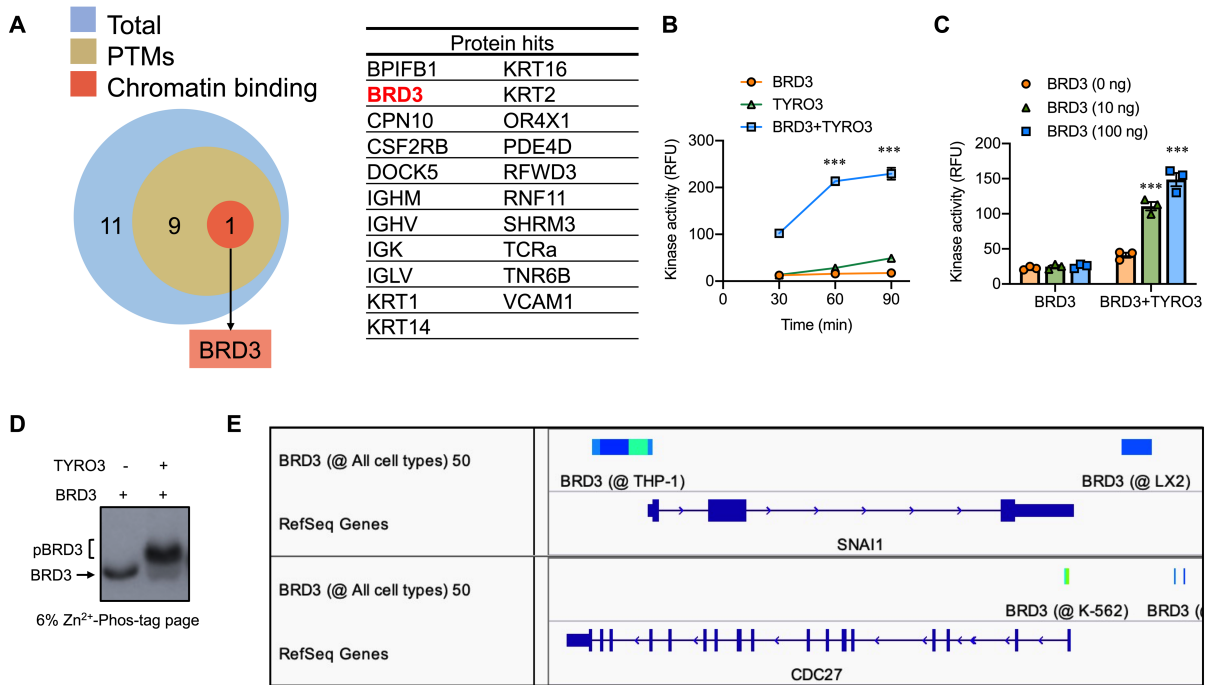
Fig. S6.

Nuclear TYRO3 interacts with BRD3.

(**A**) Functional enrichment analysis for nuclear interactor protein identified upon expression of ICD-TYRO3 in CCD-841CoN cells (PXD identifier PXD029743). PTMs: post-translational modifications. (**B**) The kinase activity of TYRO3 (100 ng) in phosphorylating BRD3 (200 ng) was measured at different time points. ***: $P < 0.001$. (**C**) The kinase activity of TYRO3 (100 ng) in phosphorylating BRD3 (0, 10, and 100 ng) measured at 1.5 hours. ***: $P < 0.001$. (**D**) Western blot shows phosphorylated BRD3 (pBRD3) is separated from unphosphorylated BRD3 when analyzed by 6% Zn^{2+}- Phos-tag™ SDS-PAGE. (**E**) Potential target genes of BRD3 were analyzed by ChIP-Atlas tool.

A

SNAI1 mRNA

siCtrl	-	+	-
siBRD3	-	-	+
ICD-TYRO3	+	-	+

***

B

SNAI1 mRNA

siCtrl	-	+	-
siBRD4	-	-	+
ICD-TYRO3	+	-	+

*** ***

C

siCtrl	-	-	+	-
siBRD3	-	-	-	+
ICD-TYRO3	-	+	-	+

SNAI1 ⎯35
β-actin ⎯45

SNAI1/β-actin

**

siCtrl	-	+	-
siBRD3	-	-	+
ICD-TYRO3	+	-	+

D

siCtrl	+	+	+	-	-	-
siBRD4	-	-	-	+	+	+

SNAI1 ⎯35
β-actin ⎯45

SNAI1/β-actin

*** *** *** ***

	Ctrl	TYRO3	ICD	Ctrl	TYRO3	ICD
siCtrl	+	+	+	-	-	-
siBRD4	-	-	-	+	+	+

E

SNAI1 mRNA

*** *** ***

sgCtrl	-	+	-
sgBRD4	-	-	+
ICD-TYRO3	+	+	+

F

sgCtrl	-	-	+
sgBRD4	-	-	-
ICD-TYRO3	-	+	+

SNAI1 ⎯35
BRD4 ⎯230 ⎯180
β-actin ⎯45

SNAI1/β-actin

** ** **

sgCtrl	-	-	+
sgBRD4	-	-	-
ICD-TYRO3	-	+	+

G

GFP | ICD-TYRO3-GFP
sgCtrl | sgBRD3 | sgBRD4

◄ Membrane ◄

Upper side

Lower side

CD31/GFP

Transendothelial migration cells/field

***

GFP, sgCtrl, sgBRD3, sgBRD4
ICD-TYRO3-GFP

H

TYRO3

Veh

5-FU

RVX-208

5-FU+ RVX-208

5-FU	-	+	-	+
RVX-208	-	-	+	+
Number	6	7	6	7
LN metastasis (%)	66.7	42.9	0	0
Liver metastasis (%)	50	28.6	0	0

I

GFP

sgCtrl-ICD-GFP

sgBRD3-ICD-GFP

sgBRD4-ICD-GFP

Group	GFP	sgCtrl-ICD-GFP	sgBRD3-ICD-GFP	sgBRD4-ICD-GFP
Number	6	6	6	5
LN metastasis (%)	0	66.7	0	60
Liver metastasis (%)	0	50	0	60

11

Fig. S7.

BRD3 mediates nuclear TYRO3's pathological functions.

(**A, B**) Results of real-time RT-qRCR show the expression of SNAI1 mRNA in *BRD3* or *BRD4* knockdown with or without ICD-TYRO3 overexpression. ***: $P < 0.001$. (**C, D**) Representative Western blots (left panel) and quantified results (right panel) show SNAI1 in HCT116 cells with *BRD3* (**C**) or *BRD4* (**D**) knockdown with or without ICD-TYRO3 overexpression. Statistical significance was calculated using two-way ANOVA and post-hoc Tukey's tests, **: $P < 0.01$, ***: $P < 0.001$. (**E**) Results of real-time RT-qRCR show the expression of SNAI1 mRNA in stable ICD-TYRO3 overexpression HCT-116 cells with (sgBRD4) or without (sgCtrl) *BRD4* knockout. ***: $P < 0.001$. (**F**) Representative Western blot (left panel) and quantified result (right panel) show SNAI1 and BRD4 in HCT116 cells with (sgBRD4) or without (sgCtrl) *BRD4* knockout. Statistical significance was calculated using two-way ANOVA and post-hoc Tukey's tests, **: $P < 0.01$. (**G**) Representative confocal images (left panel) and quantified data (right panel, n = 3) showed the HCT116 transendothelial migration. CD31: endothelial cells (red); yellow dash lines: transwell filters; arrowheads: upper and lower sides of the filters. Scale bar: 10 μm. Asterisks indicate statistical differences in intragroup comparison and pound signs indicate statistical differences in intergroup comparison, *** and ###: $P < 0.001$. (**H**) Gross view of ceca injected with HCT116 cells stably express TYRO3-GFP treated with vehicle, 5-FU, RVX-208, or RVX-208+5-FU for one month. Tumor region was circled with red dashed line (upper panel). Lower panel shows percentage of mice with lymph node and liver metastasis. (**I**) Gross view of ceca injected with HCT116 cells stably express GFP or ICD-TYRO3-GFP with control sgRNA (sgCtrl), BRD3 sgRNA (sgBRD3), or BRD4 sgRNA (sgBRD4) for 1 month. Tumor region was circled with red dashed lines (upper panel). Lower panel shows percentage of mice with lymph node and liver metastasis.

Table S1.

List of primer sequences used in this paper

Primer ID	Sequence (5' to 3')
TYRO3-mNLS F	CCTCATCCTGCTTCGAAAGGCAGCGAAAGAGACGCGGTTTGGG
TYRO3-mNLS R	CCCAAACCGCGTCTCTTTCGCTGCCTTTCGAAGCAGGATGAGG
TYRO3-mNES F	CTTGGGCATCAGCGATGAAGCAAAGGAAAAAGCGGAGGATGTGCTCATCCCAG
TYRO3-mNES R	GAACCCGTAGTCGCTACTTCGTTTCCTTTTTCGCCTCCTACACGAGTAGGGTC
TYRO3-KD F	CCTTTGTGAAAGTGGCTGTGGCGATGCTGAAAGCTG
TYRO3-KD R	CAGCTTTCAGCATCGCCACAGCCACTTTCACAAAGG
TYRO3-mMMP2 F	GTGACGGCTGCTGTCCGGGCCCTCATCCTGCTTCG
TYRO3-mMMP2 R	CGAAGCAGGATGAGGGCCCGGACAGCAGCCGTCAC
ICD-TYRO3 F	AAAGATATCCCGATGCTGGCCCTCATCCTGCTTCG
ICD-TYRO3 R	GATGGCTGGCAACTAGAAGG
ChIP qPCR_*SNAI1* F	GGAGACGAGCCTCCGATT
ChIP qPCR_*SNAI1* R	GCCGCCAACTCCCTTAAGTA
ChIP qPCR_*CDC27* F	GGCTGAAGGCGTGGCTG
ChIP qPCR_*CDC27* R	CGAGCGGGACACGGGAATAC
ChIP qPCR_Control F	CATTTCCGGGAGGACCTGA
ChIP qPCR_Control R	GAGGTGAGAGGAGGCTTC
RT-qPCR_*SNAI1* F	GCGAGCTGCAGGACTCTAAT
RT-qPCR_*SNAI1* R	GGACAGAGTCCCAGATGAGC
RT-qPCR_*GAPDH* F	ACCCAGAAGACTGTGGATGG
RT-qPCR_*GAPDH* R	TCTAGACGGCAGGTCAGGTC
sgBRD3 Sense	CACCGCAAAGGTCGGAAGCCGGCTG
sgBRD3 Antisense	AAACCAGCCGGCTTCCGACCTTTGC
sgBRD4 Sense	CACCGTAAGATCATTAAAACGCCTA
sgBRD4 Antisense	AAACTAGGCGTTTTAATGATCTTAC